MJFAS
Malaysian Journal of Fundamental and Applied Sciences

Noranuar *et al.* | Malaysian Journal of Fundamental and Applied Sciences, Vol. 20 (2024) 444-454

RESEARCH ARTICLE

Impact of Aluminum Oxide & Silicon Dioxide on Nanofluid Flow Over a Stretching Sheet with Heat Transfer: Analytical Solution

Wan Nura'in Nabilah Noranuar[a], Ahmad Qushairi Mohamad[a*], Lim Yeou Jiann[a], Sharidan Shafie[a], Mohd Anuar Jamaludin[b]

[a]Department of Mathematical Sciences, Faculty of Science, Universiti Teknologi Malaysia, 81310 Johor Bahru, Johor, Malaysia; [b]Department of Mathematics, Universiti Pertahanan Nasional Malaysia, 57000, Kuala Lumpur, Malaysia

Abstract A stretchable surface is one of the products features that numerous industrial and engineering field has been taken into consideration due to of its benefit. However, most of the fluid mechanic simulation for stretchable surface has been solved numerically and there is very limited theoretical study discovering this problem. Therefore, the present study investigated the convective Casson nanofluid flow and heat transfer over a linear stretching sheet. The aluminum oxide (Al_2O_3) and silicon dioxide (SiO_2) are considered. The analytical resolution of the governing problem yields velocity and temperature solutions using the Laplace transform method. Graphical representation illustrates how nanoparticle volume fraction affects velocity and temperature distribution profiles. Higher nanoparticle volume fractions slow down nanofluid flow and elevate temperature profiles. This investigation establishes a robust foundation for future research utilizing numerical methods.

Keywords: Stretching sheet, Nanofluid, Casson fluid, Laplace transform method, Heat transfer.

Introduction

Study of boundary layer flow across a stretching sheet with heat transfer analysis has grabbed many concerned of researchers due to their substantial application in industrial and engineering fields. A stretchable surface is known as an area supported at an edge and its movement occurs when another edge is pulled. The sheet appearance is formed when the material is melted and expanded to the desired size [1]. These characteristics of products can be found in many industrial processes, including paper production, metal packaging and aluminium bottle manufacturing processes, hot and wire rolling, and manufacture of glass fibre. Initially, Crane [2] is the pioneer to the study of flow across a stretchable surface. Over the years, the concept of stretching sheet in fluid flow analysis has grabbed many concerned of researchers, which encourages them to extend the study with various physical aspects, considering different types of fluid model, complicated problem geometry, and varies effects. Amongst them are Das *et al*. [3], who investigated the magneto-nanofluid across an accelerating stretching sheet, Manjunatha *et al*. [4] examined the heat transport of tri-hybrid nanofluid model, Sreedevi *et al*. [5] worked on mass and heat transfer analysis for MHD flow, and Hosseinzadeh *et al*. [6] studied the impact of inconsistent heat generation and absorption for convective nanofluid flow. Due to the involvement of complicated non-linear differential equations, all this research has been numerically resolved by means of Runge Kutta Fehlberg method and finite difference method. In other hands, Hamad [7] performed the analytical study to examine the viscous MHD nanofluid flow but applying WhittakerM function and hypergeometric function in their solution.

***For correspondence:**
ahmadqushairi@utm.my

Received: 15 Nov. 2023
Accepted: 4 Feb. 2024

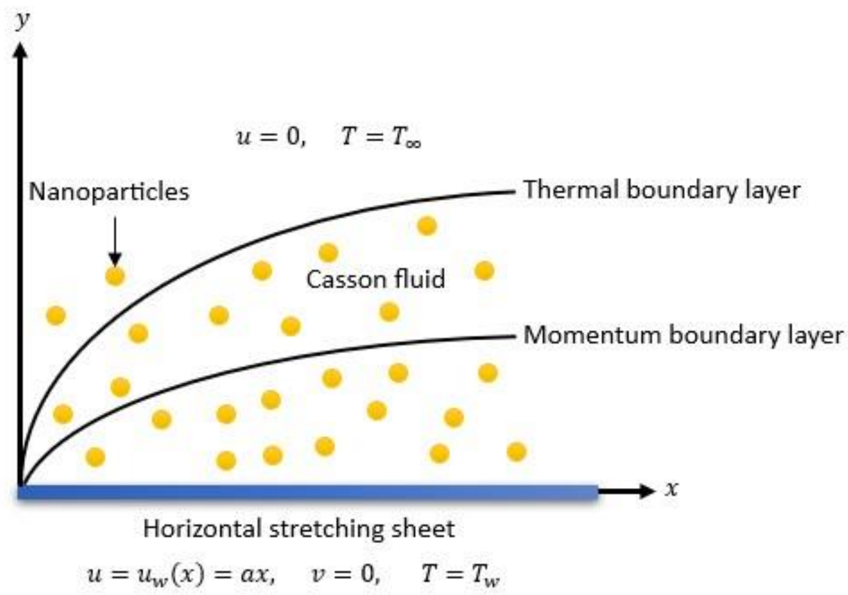

Figure 1. Flow geometry

Based on the above-mentioned study, there is no researcher conducted this investigation analytically by using the Laplace transform method. In fact, the analytical study is important to be emphasized due to its significant as the benchmark for other numerical and experimental work and can save the cost and time to conduct the experiment. Among the researchers who applied this method to solve the stretching sheet problem are Ebaid and Al Sharif [8], examining the magnetic field on the heat transfer and boundary layer flow of viscous nanofluid past a linear stretching sheet with carbon nanotubes as the nanoparticles. Saleh *et al*. [9] extended the previous study by introducing the consequence of suction and injection in the system. Both studies applied the Laplace transform method to obtain the exact solution for heat transfer and expressed the solution in the generalized incomplete gamma function. A viscoplastic hybrid nanofluid flow by Hussanan *et al*. [10], a viscoelastic fluid flow by Afridi *et al*. [11] and a Jeffery fluid flow by Qasim [12] were studied across a surface with linear stretched, generating the exact thermal solution in hypergeometric function. Lu *et al*. [13] explored the characteristics of dissipative nanofluid flow with heat transfer incorporating the boundary's transpiration effect. In this study, the nanofluid correlation by Tiwari and Das model was employed. Maranna *et al*. [14] investigated the influences of radiation and magnetic field on the Newtonian based carbon nanotubes nanofluid over a linearly stretching sheet. The analytical study of non-linear stretching sheet was also done by Aly and Ebaid [15] for a Marangoni boundary layer flow in a porous material. The slip flow of hybrid nanofluid past through porous stretching surface with the effect of chemical reaction was investigated by Mahabaleshwar *et al*. [16]. Without nanoparticles impacts, Afridi *et al*. [17] acquired the exact solution for MHD Newtonian fluid flow in the presence of Joule heating and viscous dissipation. As an extension of the study, Chen *et al*. [18] shifted to Brinkman fluid model while considering the porosity effect. Following to the reviewed literature, most of the stretching sheet study were carried out for a Newtonian (viscous) nanofluid model and there is no investigation is done for a Casson nanofluid model. The most related study for nanofluid flow past stretching sheet considering Casson fluid model was carried out by Bhattacharyya *et al*. [19] but the authors have solved only for the momentum equation without considering nanoparticles effect. Considering this deficiency, the current study takes the opportunity to derive the governing momentum and energy equations and solve the problem by means of the Laplace transform method. In other words, this paper investigated the incompressible steady Casson nanofluid flow and heat transfer across a stretching sheet. The problem is governed by the partial differential momentum and energy equations associated with initial and linear stretchable sheet boundary condition. The Laplace transform is used to generate the solutions and further analyze using graphical results.

Mathematical Formulation

An incompressible Casson nanofluid flow moving steadily over a linear stretching sheet is considered as illustrated in Figure 1. The sheet is horizontally stretched with the velocity $u = ax$, where a is a constant, along x-axis, while y-axis is considered perpendicular to the sheet. The nanofluid with different base fluids, which are water and sodium alginate, respectively composing different metal oxide nanoparticles (Al_2O_3 and SiO_2) are considered. It is supposed that no slip occurs between the nanoparticles and the base fluid, and that they are both in thermal equilibrium. The thermal physical features for base fluids and nanoparticles are shown in Table 1. The constant T_w represent the temperature at the stretching surface, while the ambient temperature T_∞ represent the temperature for y approaches to infinity ($y \to \infty$).

Table 1. Thermal physical features for base fluids and nanoparticles [20, 21]

Base fluid / nanoparticles	$\rho(Kgm^{-1})$	$C_p(JKg^{-1}K^{-1})$	$k(Wm^{-1}K\hat{}-1)$
Water	997.1	4179	0.613
Sodium alginate	989	4175	0.6376
Al_2O_3	3970	765	40
SiO_2	2200	745	1.4

The stress tensor defining the rheological state for Casson fluid is expressed by the following condition [22, 23, 24], which is

$$\tau_{ij} = \{\left(\mu_b + \frac{\tau_y}{\sqrt{2\pi}}\right)2e_{ij}\pi > \pi_c, \left(\mu_b + \frac{\tau_y}{\sqrt{2\pi}}\right)2e_{ij}\pi < \pi_c, \tag{1}$$

where μ_b is the plastic dynamic, τ_y is the yield stress of non-Newtonian Casson fluid, π_c is the critical value of the deformation rate, $\pi = e_{ij}e_{ij}$ with e_{ij} is the $(i,j)^{th}$ element of the deformation rate. Considering the above suppositions, the boundary layer problem is represented by the following partial differential equations (PDEs) as

$$\frac{\partial u}{\partial x} + \frac{\partial v}{\partial y} = 0, \tag{2}$$

$$u\frac{\partial u}{\partial x} + v\frac{\partial u}{\partial y} = \nu_{nf}\left(1 + \frac{1}{\beta}\right)\frac{\partial^2 u}{\partial y^2}, \tag{3}$$

$$(\rho C_p)_{nf}\left(u\frac{\partial T}{\partial x} + v\frac{\partial T}{\partial y}\right) = k_{nf}\frac{\partial^2 T}{\partial y^2}. \tag{4}$$

The specified conditions for initial and boundary are

$$u = u_w(x) = ax,\ v = 0; \quad T = T_w; \quad y = 0, \tag{5}$$

$$u = 0; \quad T = T_\infty; \quad y \to \infty, \tag{6}$$

where $\beta = {}^{\mu\sqrt{2\pi_c}}\!/_{\tau_y}$ is Casson fluid parameter. The above nanofluid terms, which are kinematic viscosity ν_{nf}, density ρ_{nf}, specific heat capacitance $(C_p)_{nf}$, and thermal conductivity k_{nf}, are given as

$$\begin{gathered}\rho_{nf} = (1-\phi)\rho_{nf} + \phi\rho_s, \quad \nu_{nf} = \frac{\mu_{nf}}{\rho_{nf}},\\ \mu_{nf} = \frac{\mu_f}{(1-\phi)^{2.5}},\\ (\rho C_p)_{nf} = (1-\phi)(\rho C_p)_f + (\rho C_p)_s,\\ k_{nf} = k_f\left\{\frac{k_s + 2k_f - 2\phi(k_f - k_s)}{k_s + 2k_f + 2\phi(k_f - k_s)}\right\},\end{gathered} \tag{7}$$

where the subscript s, f, nf are nanoparticles, base fluid, nanofluid, and ϕ is the nanoparticle volume fraction.

By following the procedures of non-dimensionlizing and similarity transformations mentioned in Hamad [7], it maps to the following non-linear differential equations

$$\left(1+\frac{1}{\beta}\right)f'''(\eta)+\alpha[f(\eta)f''(\eta)-f(\eta)'^2]=0, \tag{8}$$

$$\tau\theta''(\eta)+\ f(\eta)\theta'(\eta)=0, \tag{9}$$

where

$$\alpha=(1-\phi)^{2.5}\left[1-\phi+\phi\left(\frac{\rho_s}{\rho_f}\right)\right], \tag{10}$$

$$\tau=\frac{1}{\mathrm{Pr}}\left(\frac{k_{nf}}{k_f}\right)\left(\frac{1}{\left(1-\phi+\phi\left(\frac{\rho_s}{\rho_f}\right)\right)}\right). \tag{11}$$

The transformed boundary conditions for dimensionless stream function f and temperature θ are

$$f(\eta)=0,\quad f'(\eta)=1,\quad \theta(\eta)=1;\quad \eta=0, \tag{12}$$

$$f'(\eta)=1,\quad \theta(\eta)=0;\quad \eta\to\infty. \tag{13}$$

Here, $\mathrm{Pr}={(\rho C_p)_f \nu_f}/{k_f}$ defines Prandtl number.

Solution of Problem

Exact Solution of the Flow

Assuming that the exact solution for Equation (8) subjects to Equation (12) can be deduced as given in Hamad [7], Ebaid and Al Sharif [8], Aly and Ebaid [15], Bhattacharyya *et al*. [19]

$$f(\eta)=a_1+a_2e^{-b\eta}. \tag{14}$$

The constant a_1 and a_2 are obtained as

$$a_1=\frac{1}{b},\quad a_2=-\frac{1}{b}. \tag{15}$$

where b can be found by substituting Equation (14) and (15) into Equation (8), as

$$b=\sqrt{\frac{\alpha\beta}{\beta+1}}. \tag{16}$$

Exact Solution of Heat Transfer

For heat transfer, Equation (14) and (15) are inserted to Equation (9), which maps to

$$\tau\theta''(\eta)+\left(\frac{1}{b}-\frac{1}{b}e^{-b\eta}\right)\theta'(\eta)=0. \tag{17}$$

After that, the independent variable t=exp^(-beta*n) (Saleh *et al*. [9]) is used to transform Equation (17) to

$$t\theta''(t)+\ (p-qt)\theta'(t)=0, \tag{18}$$

where $p=1-\frac{1}{\tau b^2}$ and $q=-\frac{1}{\tau b^2}$, and associated with conditions for boundary

$$\theta(0)=0,\quad \theta(1)=1. \tag{19}$$

Next, employing Equation (18) with the Laplace transformation yields

$$s(p-s)\Theta(s)+[p+(q-2)s]\Theta(s)=0, \tag{20}$$

where $\Theta(s)$ is the Laplace transform of $\theta(t)$. Then, integrating Equation (20) gives

$$\Theta(s) = \frac{m}{s(s-p)^{1-q}}, \tag{21}$$

where m is a constant of integration. Equation (21) are then imposed with the inverse Laplace transform and obtains

$$\theta(t) = \frac{m}{\Gamma(1-q)}(t^{-q}e^{pt}), \quad q < 1, \tag{22}$$

which automatically satisfied the boundary $\theta(0) = 0$. Following the details of convolution property, mentioned in Saleh *et al*. [9], Equation (22) accordingly becomes

$$\theta(t) = \frac{m}{\Gamma(1-q)}\left(-\frac{1}{p}\right)^{1-q}\Gamma(1-q,0,-pt). \tag{23}$$

Implementing the other boundary condition $\theta(1) = 1$ obtains m as

$$m = \frac{\Gamma(1-q)}{\left(-\frac{1}{p}\right)^{1-q}\Gamma(1-q,0,-p)}. \tag{24}$$

Therefore, the exact solution for $\theta(t)$ is given in the following generalized incomplete gamma function form

$$\theta(t) = \frac{\Gamma(1-q,0,-pt)}{\Gamma(1-q,0,-p)}, \tag{25}$$

which can be written in term of η as

$$\theta(\eta) = \frac{\Gamma(1-q,0,-pe^{-b\eta})}{\Gamma(1-q,0,-p)}. \tag{26}$$

It was concluded that employing the Laplace transform as a solution tool leads to simpler special functions, whereas alternative techniques, as exemplified by Hamad [7], result in more complex special functions.

Physical Quantities

Additionally, the Casson nanofluid flow over a linearly stretching sheet is governed by the physical quantities, which are respectively defined as:

Skin friction coefficient (Cf_x) and local Nusselt number (Nu_x):

$$Cf_x = \frac{\tau_w}{\rho u_w^2}, \quad Nu_x = \frac{xq_w}{k(T_w - T_\infty)}, \tag{27}$$

where τ_w is the wall shear stress and q_w is the wall heat flux, which are defined as

$$\tau_w = \mu_b\left(1 + \frac{1}{\beta}\right)\left(\frac{\partial u}{\partial y}\right)\bigg|_{y=0}, \quad q_w = -k\left(\frac{\partial T}{\partial y}\right)\bigg|_{y=0}. \tag{28}$$

Incorporating Equations (6) and (14) in Hamad [7], the surface drag force and the rate of heat transfer forms as

$$Re_x^{\frac{1}{2}}Cf_x = \left(1 + \frac{1}{\beta}\right)f''(0), \quad Re_x^{\frac{1}{2}}Nu_x = -\theta'(0), \tag{29}$$

where $Re_x^{\frac{1}{2}} = \frac{u_w(x)}{v}$ is the local Reynolds number.

Results and Discussion

An investigation of Casson nanofluid flow and heat transfer across a linear stretching sheet by applying the Laplace transform approach has been conducted in this paper. To comprehend the propagation of flow and transportation of heat, the graphical results are generated using Matlab software with different values of dimensionless factors which are nanoparticles volume fraction ϕ and Casson parameter β. The comparative study is done by considering two types of metal oxide nanoparticles, which are Aluminium oxide Al_2O_3 and Silicon dioxide SiO_2, that respectively suspended in two different base fluids, which are water and sodium alginate. The velocity solution obtained in this present study are compared to the previous study by Bhattacharyya *et al*. [19], by letting $\phi = 0$ in the present study. The comparison, illustrated in Figure 2, shows that both studies generate an identical solution, which confirmed the validity of the present study.

The effect of nanoparticles volume fraction ϕ on the velocity profile is illustrated in Figure 3. The increase of ϕ results a reduction in velocity profile. It is because increasing ϕ causes the nanofluid becomes more viscous and thicker, which produces a higher viscous force on the flow and the velocity becomes slower. The velocity profile is further analysed for the impact of Casson fluid parameter β as demonstrated in Figure 4. It is observed that the velocity reduces by increasing β. This effect is because of the fluid plasticity becomes greater when β is increased, and eventually decreases momentum boundary layer as well as velocity profile.

Figure 5 discusses a comparative nanofluid when $\phi = 0.02$. The comparison, for the case of base fluid, shows that the magnitude of velocity for water based nanofluid is higher than sodium alginate (SA) based nanofluid, which is because SA based nanofluid is denser than water based nanofluid. The similar finding with its reason was also discussed in the study of Raza *et al*. [25]. Furthermore, for the case of nanoparticles, because of higher density of Al_2O_3, it is found that the velocity for Al_2O_3 nanofluid is slower than SiO_2 nanofluid. Moreover, it is also observed that SiO_2 nanofluid has thicker momentum boundary layer compared to Al_3O_2 nanofluid.

The contribution of nanoparticle volume fraction ϕ on the temperature profile is demonstrated in Figure 6. Physically, the nanoparticles possess an outstanding thermal conductivity compared to the conventional base fluid, whereby its addition to the base fluid will eventually improve the fluid thermal conductivity and increase the thickness of thermal boundary layer. From this figure, it clearly observed that heat profile increases with ever growing ϕ values, due to the thermal conductivity of nanofluid is enhanced and the more heat has been absorbed into the system which finally grows the temperature profile as well as the thermal boundary layer. Besides, due to Al_2O_3 nanoparticle has higher thermal conductivity, it is observed that nanofluid with Al_2O_3 nanoparticle exhibits a prominent temperature profile compared to nanofluid with SiO_2 nanoparticle.

The variation of skin friction coefficient and Nusselt number are tabulated in Tables 2 and 3, respectively. In Table 2, the provocation of ϕ values for nanofluid with Al_2O_3 nanoparticles declines the skin friction coefficient. Meanwhile, the opposite trend is observed for nanofluid with SiO_2 nanoparticles, where an elevated skin friction is reported as values of ϕ increases. This is equivalent to augmenting surface drag force that can increase the flow resistance and accordingly results a diminution of velocity by ϕ values. Besides, an upsurge in β values raises the skin friction for all types of nanofluid. This effect signifies to enhancement drag force at the surface, which consequently leads to a decreasing velocity profiles. In Table 3, the provocative ϕ values results an increase in Nusselt number, indicating to the enhancement of heat transfer rate. This effect is influenced by the boosted nanofluid thermal conductivity when the ϕ values are raised, which cause a rapid heat transmission by nanofluid. Moreover, when comparing the thermal conductivity between nanofluids, it is unveiled that the higher thermal conductivity of Al_2O_3 nanoparticles compared to SiO_2 nanoparticles causes the Al_2O_3 nanofluid to transfer heat quickly. This is significantly indicated by prominent values of Nusselt number by Al_2O_3 nanofluid.

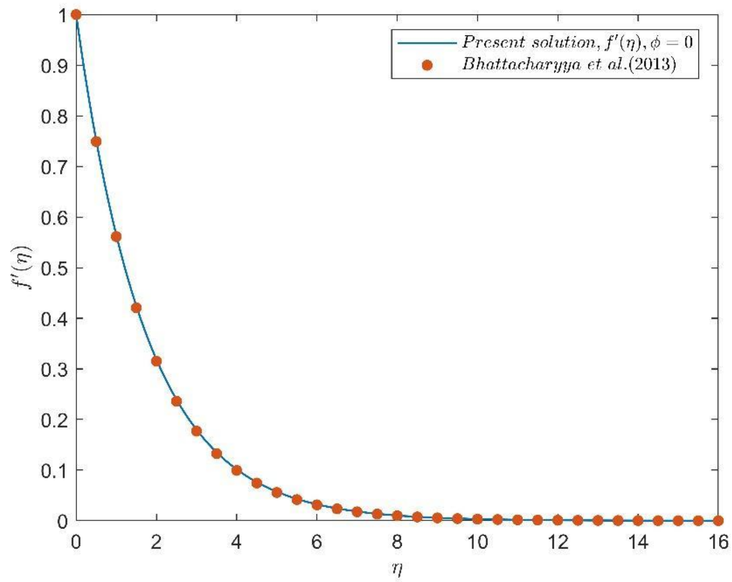

Figure 2. Verification of the present study

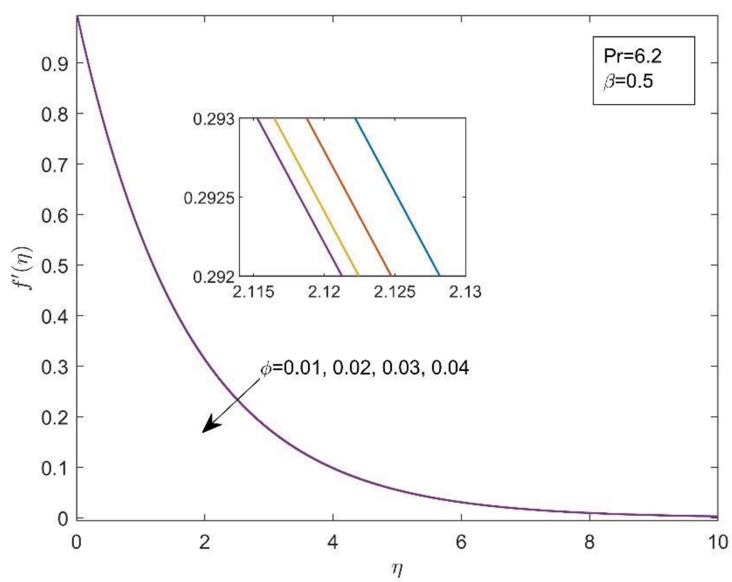

Figure 3. Graph of velocity $f'(\eta)$ vs η for different ϕ values

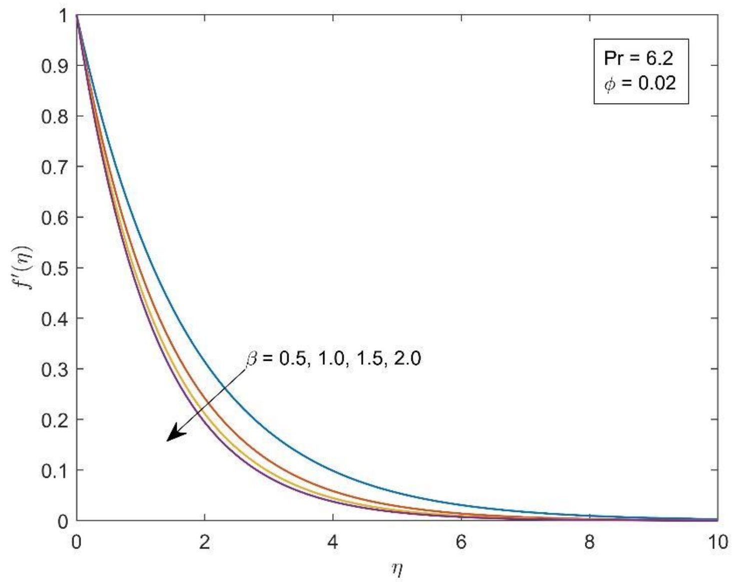

Figure 4. Graph of velocity $f'(\eta)$ vs η for different β values

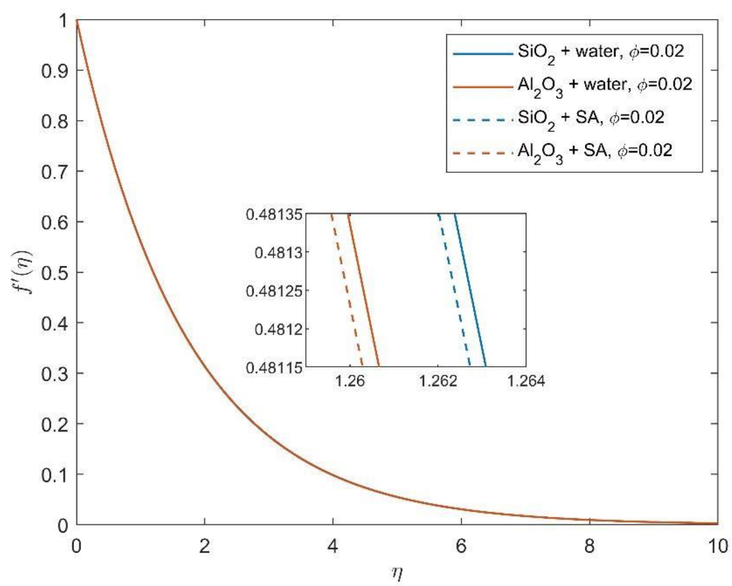

Figure 5. Comparison of different nanofluids when $\phi = 0.02$.

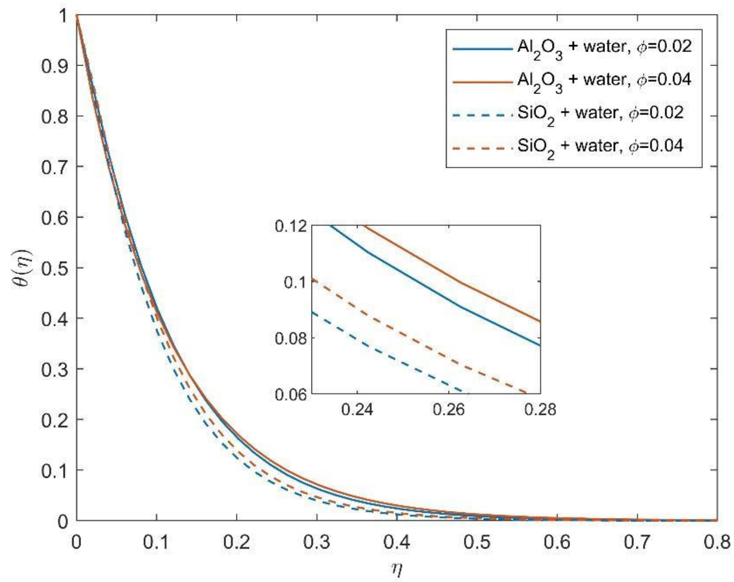

Figure 6. Comparison of different nanofluids with when $\phi = 0.02$ and $\phi = 0.04$.

Table 2. Variation of skin friction

ϕ	β	$\left(1+\frac{1}{\beta}\right)f''(0)$			
		Al_2O_3 +water	SiO_2 +water	Al_2O_3 +SA	SiO_2 +SA
0.00	0.5	-54.7723	-54.7723	-53.7723	-54.7723
0.01	0.5	-54.8895	-54.4141	-54.8976	-54.4186
0.02	0.5	-54.9769	-54.0475	-54.9926	-54.0564
0.04	0.5	-55.0661	-53.2898	-55.0958	-53.3068
0.02	1.0	-44.8885	-44.1296	-44.9013	-44.1368
0.02	1.5	-40.9774	-40.2847	-40.9891	-40.2912
0.02	2.0	-38.8745	-38.2174	-38.8856	-38.2236

Table 3. Variation of Nusselt number

ϕ	β	$-\theta'(0)$			
		Al_2O_3 +water	SiO_2 +water	Al_2O_3 +SA	SiO_2 +SA
0.00	0.5	-5.5267	-5.5267	-5.7267	-5.7267
0.01	0.5	-5.2533	-5.4467	-5.4400	-5.6333
0.02	0.5	-4.9933	-5.3667	-5.1733	-5.5467
0.04	0.5	-4.5067	-5.2000	-4.6600	-5.3667
0.02	1.0	-10.5600	-11.4600	-10.9333	-11.8467
0.02	1.5	-14.0733	-15.2667	-14.5533	-15.7667
0.02	2.0	-16.4400	-17.8133	-16.9867	-18.3867

Conclusions

In this paper, a comprehensive study on steady Casson nanofluid flow past through a linear stretching sheet has been carried out. The exact solution using the Laplace transformation has been achieved to study the fluid flow and thermal features of Al_2O_3 and SiO_2 nanofluids with a Casson fluid model. Some useful conclusions are made as the following.

- The nanofluid velocity profiles decelerates with superior ϕ.

- While an ascend of β values reduce the nanofluid velocity profiles.
- An increment of ϕ values rise the temperature profiles of nanofluid.
- The velocity profiles for SiO_2 nanofluid precede the velocity profiles of Al_2O_3 nanofluid.
- Velocity water based nanofluid precedes the velocity SA based nanofluid.
- Upsurge values of ϕ enhances skin friction coefficient for SiO_2 nanofluid while the opposite effect is observed for Al_2O_3 nanofluid.
- Growing β values enhances skin friction coefficient for all types of nanofluid.
- Rate of heat transfer increases with an upsurge ϕ values.

Conflicts of Interest

The author(s) declare(s) that there is no conflict of interest regarding the publication of this paper.

Acknowledgment

This research was funded by Universiti Teknologi Malaysia under Matching Grant Scheme R.J130000.7354.4B748 and Q.J130000.3054.03M77.

References

[1] Jafar, A. B., Shafie, S., Ullah, I., Safdar, R., Jamshed, W., Pasha, A. A., Rahman, M. M., Hussain, S. M., Rehman, A., El Din, E., & Eid, M. R. (2022). Mixed convection flow of an electrically conducting viscoelastic fluid past a vertical nonlinearly stretching sheet. *Sci Rep., 12*(1), 14679. Doi:10.1038/s41598-022-18761-0

[2] Crane, L. J. (1970). Flow past a stretching plate. *Kurze Mitteilungen - Brief Reports - Communications br~ves*, 21.

[3] Das, S., Chakraborty, S., Jana, R. N., & Makinde, O. D. (2015). Entropy analysis of unsteady magneto-nanofluid flow past accelerating stretching sheet with convective boundary condition. *Applied Mathematics and Mechanics, 36*(12), 1593-1610. Doi:10.1007/s10483-015-2003-6.

[4] S. Manjunatha, V. P., B.J. Gireesha, & Ali J. Chamkha. (2022). Theoretical study of convective heat transfer in ternary nanofluid flowing past a stretching sheet. *Journal of Applied and Computational Mechanics, 8*(4), 1279-1286. Doi:10.22055/JACM.2021.37698.3067.

[5] Sreedevi, G., Raghavendra Rao, R., Prasada Rao, D. R. V., & Chamkha, A. J. (2016). Combined influence of radiation absorption and Hall current effects on MHD double-diffusive free convective flow past a stretching sheet. *Ain Shams Engineering Journal, 7*(1), 383-397. Doi:10.1016/j.asej.2015.11.024.

[6] Hosseinzadeh, K., Afsharpanah, F., Zamani, S., Gholinia, M., & Ganji, D. D. (2018). A numerical investigation on ethylene glycol-titanium dioxide nanofluid convective flow over a stretching sheet in presence of heat generation/absorption. *Case Studies in Thermal Engineering, 12*, 228-236. Doi:10.1016/j.csite.2018.04.008.

[7] Hamad, M. A. A. (2011). Analytical solution of natural convection flow of a nanofluid over a linearly stretching sheet in the presence of magnetic field. *International Communications in Heat and Mass Transfer, 38*(4), 487-492. Doi:10.1016/j.icheatmasstransfer.2010.12.042.

[8] Ebaid, A., & Al Sharif, M. A. (2015). Application of Laplace transform for the exact effect of a magnetic field on heat transfer of carbon nanotubes-suspended nanofluids. *Zeitschrift für Naturforschung A, 70*(6), 471-475. Doi:10.1515/zna-2015-0125.

[9] Saleh, H., Alali, E., & Ebaid, A. (2018). Medical applications for the flow of carbon-nanotubes suspended nanofluids in the presence of convective condition using Laplace transform. *Journal of the Association of Arab Universities for Basic and Applied Sciences, 24*(1), 206-212. Doi:10.1016/j.jaubas.2016.12.001.

[10] Hussanan, A., Qasim, M., & Chen, Z. M. (2020). Heat transfer enhancement in sodium alginate based magnetic and non-magnetic nanoparticles mixture hybrid nanofluid. *Physica A: Statistical Mechanics and its Applications*, *550*, 123957.

[11] Afridi, M. I., Qasim, M., & Makinde, O. D. (2019). Entropy generation due to heat and mass transfer in a flow of dissipative elastic fluid through a porous medium. *Journal of Heat Transfer*, *141*(2), 022002.

[12] Qasim, M. (2013). Heat and mass transfer in a Jeffrey fluid over a stretching sheet with heat source/sink. *Alexandria Engineering Journal*, *52*(4), 571-575.

[13] Lu, D., Afridi, M. I., Allauddin, U., Farooq, U., & Qasim, M. (2020). Entropy generation in a dissipative nanofluid flow under the influence of magnetic dissipation and transpiration. *Energies*, *13*(20), 5506.

[14] Maranna, T., Sneha, K. N., Mahabaleshwar, U. S., Sarris, I. E., & Karakasidis, T. E. (2022). An effect of radiation and MHD Newtonian fluid over a stretching/shrinking sheet with CNTs and mass transpiration. *Applied Sciences, 12*(11). Doi:10.3390/app12115466.

[15] Aly, E. H., & Ebaid, A. (2016). Exact analysis for the effect of heat transfer on MHD and radiation Marangoni boundary layer nanofluid flow past a surface embedded in a porous medium. *Journal of Molecular Liquids, 215*, 625-639. Doi:10.1016/j.molliq.2015.12.108.

[16] Mahabaleshwar, U. S., Anusha, T., Beg, O. A., Yadav, D., & Botmart, T. (2022). Impact of Navier's slip and

chemical reaction on the hydromagnetic hybrid nanofluid flow and mass transfer due to porous stretching sheet. *Sci Rep, 12*(1), 10451. Doi:10.1038/s41598-022-14692-y.

[17] Afridi, M. I., Qasim, M., & Shafie, S. (2017). Entropy generation in hydromagnetic boundary flow under the effects of frictional and Joule heating: Exact solutions. *The European Physical Journal Plus*, *132*, 1-11.

[18] Chen, Z. M., Afridi, M. I., Riaz, N., & Qasim, M. (2024). Impact of porous and magnetic dissipation on dissipative fluid flow and heat transfer in the presence of Darcy-Brinkman porous medium. *Journal of Porous Media*. *27*(3), 45-65.

[19] Bhattacharyya, K., Hayat, T., & Alsaedi, A. (2014). Exact solution for boundary layer flow of Casson fluid over a permeable stretching/shrinking sheet. *ZAMM - Journal of Applied Mathematics and Mechanics / Zeitschrift für Angewandte Mathematik und Mechanik, 94*(6), 522-528. Doi:10.1002/zamm.201200031.

[20] Alghamdi, M., Wakif, A., Thumma, T., Khan, U., Baleanu, D., & Rasool, G. (2021). Significance of variability in magnetic field strength and heat source on the radiative-convective motion of sodium alginate-based nanofluid within a Darcy-Brinkman porous structure bounded vertically by an irregular slender surface. *Case Studies in Thermal Engineering*, *28*, 101428.

[21] Khan, M. R., Pan, K., Khan, A. U., & Nadeem, S. (2020). Dual solutions for mixed convection flow of SiO_2–Al_2O_3/water hybrid nanofluid near the stagnation point over a curved surface. *Physica A: Statistical Mechanics and its Applications*, *547*, 123959.

[22] Qasim, M., & Noreen, S. (2014). Heat transfer in the boundary layer flow of a Casson fluid over a permeable shrinking sheet with viscous dissipation. *The European Physical Journal Plus*, *129*, 1-8.

[23] Qasim, M., & Ahmad, B. (2015). Numerical solution for the blasius flow in a Casson fluid with viscous dissipation and convective boundary conditions. *Heat Transfer Research*, *46*(8).

[24] Butt, A. S., Tufail, M. N., & Ali, A. (2016). Three-dimensional flow of a magnetohydrodynamic Casson fluid over an unsteady stretching sheet embedded into a porous medium. *Journal of Applied Mechanics and Technical Physics*, *57*, 283-292.

[25] Raza, A., Khan, S. U., Farid, S., Khan, M. I., Sun, T.-C., Abbasi, A., Khan, M. I., & Malik, M. Y. (2021). Thermal activity of conventional Casson nanoparticles with ramped temperature due to an infinite vertical plate via fractional derivative approach. *Case Studies in Thermal Engineering, 27*. Doi:10.1016/j.csite.2021.101191.